Random mutagenesis and silver nitrate ($AgNO_3$) based negative selection of different metallothioneins (MTs) exploring the potential for functional MT directed evolution.

Dev Vaidya, Serafina Soehianto, Diana Barreiros Jorge, Maarten Van Den Ancker, Xianliang Xu, William McKenny, Dovydas Samulionis, Zhongyi Liang, Arin Wongprommoon, Michael Stam, Nadanai Laohakunakorn & Chris French

Abstract:

Heavy-metal water pollution is a major public health and biodiversity crisis. Metallothioneins (MT) are cysteine-rich proteins involved in metal-homeostasis and heavy-metal bioaccumulation. The Edinburgh-UHAS_Ghana iDEC team is exploring the potential of MT directed evolution as a mechanism for increasing heavy-metal bioaccumulation. A silver nitrate based negative selection and mutant screening method has been developed to select MTs with higher metal binding capacity. Mutant libraries were created using error-prone PCR for four MTs of interest. A single mutant and its wild-type variant were expressed in BL21(DE3) cells and inputted into the negative selection method. Results indicated that MT expression increases the silver resistance. MTs from six species of interest were structurally modelled via Alphafold and docking simulations using silver as the ligand were performed. Conservation scores from multiple sequence alignments were used to propose functional mutation sites for all MTs of interest and site-specific mutagenic primers were made for the same.

Key Words*: Negative selection, error-prone PCR, Metallothionein, docking simulation*

1. Introduction

Humanity is nearing a water pollution-caused public health crisis (Schwarzenbach et al. 2010). From heavy metals to the spread of pathogens, human activities are endangering water health compromising both public health and biodiversity.
Water bodies in Ghana such as the Birim River have been reported to contain lead, mercury, and cadmium levels at 400, 180, and 15 times over the World Health Organization (WHO) recommended limit, respectively (Afum and Owusu, 2016). Ingestion of heavy metal-contaminated water has been associated with many health risks such as, kidney damage and neurotoxic effects. Water pollution has also led to growing concerns about heavy metal accumulation in soil and crops.
Nature bears examples in which life exists alongside heavy metals. Metallothioneins (MTs) are intracellular, cysteine-rich proteins, instrumental in metal chelation (Coyle *et al.* 2002). MTs do so, by forming metal binding motifs which utilise thiol groups on cysteine sidechains to coordinate covalent bonds with various metals (monovalent, divalent and trivalent). In aquatic invertebrates, MTs have been well studied, and are known to aid in heavy metal bioaccumulation. A wide variety of MTs from various species were chosen for this study. *Mytilus edulis* (blue mussel) was the first species in which MTs were characterised and have been well studied (Leignel and Laulier, 2006). We picked a closely related species, *M. galloprovincialis* (Mediterranean mussel) for comparison (Vergani *et al.*, 2007). *Callinectes sapidus*, an aquatic crustacean living in high heavy metal rich environments was also studied (De Martinez Gaspar Martins and Bianchini, 2009). *Danio rerio* and *Saccharomyces cerevisiae* are well-characterised model organisms, thus making their exploration relevant to ongoing research (Chan *et al.*, 2006; Butt and Ecker, 1987). *Pseudomonas fluorescens* was studied to account for potential differences in prokaryotic and eukaryotic MTs (Habjanič *et al.*, 2020; Olafson, 1984).

The goal of the study was to randomly mutagenize the chosen MTs and develop an effective selection screen to identify *E. coli* colonies recombinantly expressing MTs that bind more metal ions. This screen would work as a preliminary test for MT function in metal-bioaccumulation for applications like heavy metal bioremediation. A selection screen was designed using BL21 (DE3) *E. coli* as the expression strain. MT-expressing cells would be subjected to a toxic metal environment. Bacterial

survival was hypothesised to indicate improved metal bioaccumulation, saving bacteria from toxic environments well over their maximum inhibitory concentration (MIC).
Silver ion (Ag^{+}) is used as an antimicrobial agent in both clinical and non-clinical applications (Chopra, 2007). Silver is toxic to gram-negative bacteria like *E. coli* while also functioning as a ligand for MTs (Scheuhammer and George, 1986). Other MT ligands like zinc and copper have previously been used to understand MT ligand binding and binding affinity (Xu et al. 2018), however, we found that these metals did not exhibit usable toxicity towards *E. coli* strains to design a selection pressure. Silver is not a heavy metal nor is it a common water pollutant, however, it is a safer alternative to using lead, mercury, cadmium, or arsenic which are good ligands and common toxic pollutants.

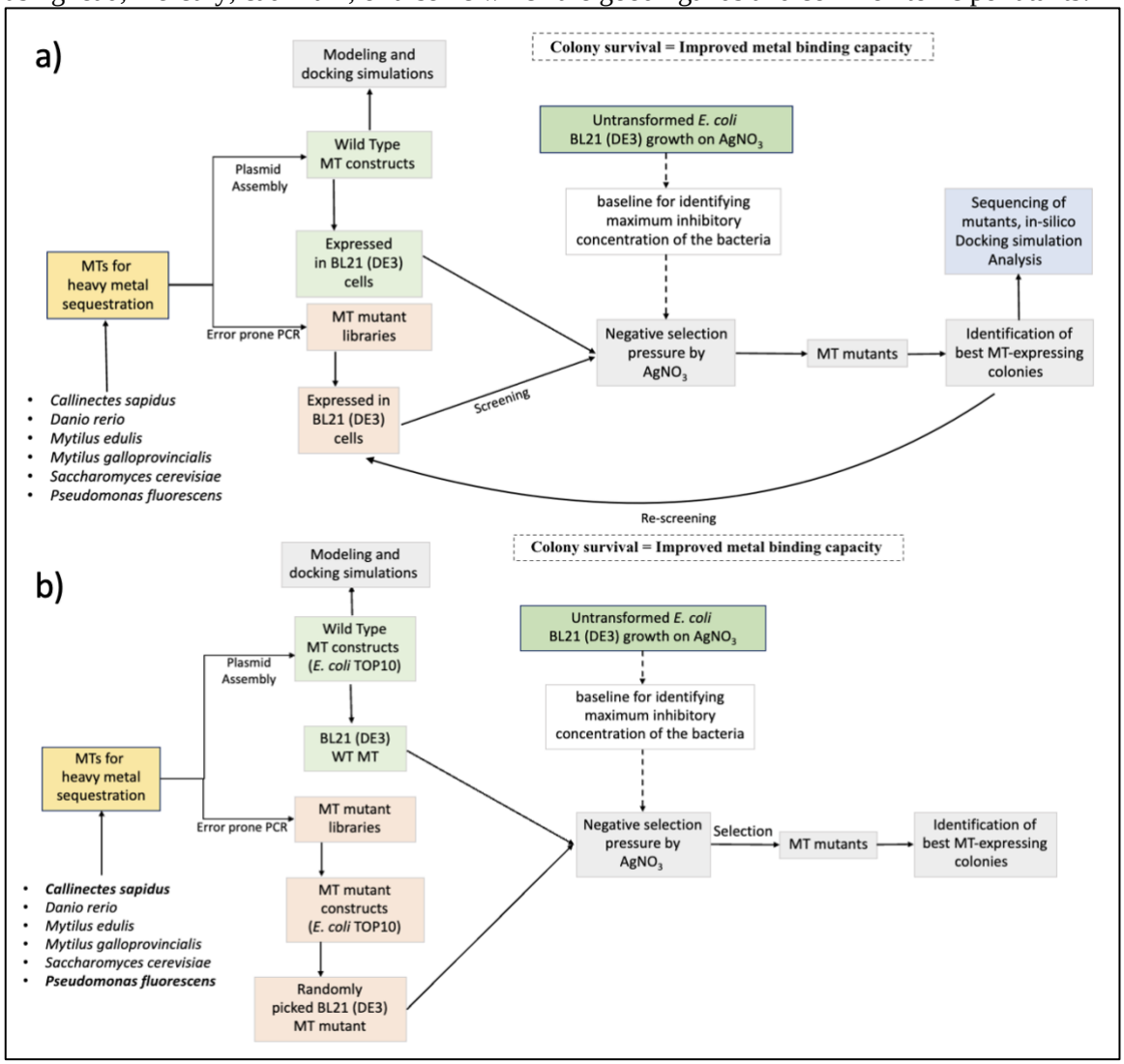

Figure 1 a) Illustrates the planned workflow including a BL21 (DE3) MT mutant screen for all six species listed above, sequencing and characterisation of mutants and comparative docking simulations. **b)** Represents, the experimental results and work highlighted in this study. It can be noted that a singular mutant was selected against its wild type (WT) variant and assembled plasmids were first expressed in an alternate *E. coli* strain (TOP10). Additionally, mutants which survived at higher $AgNO_3$ concentrations were not characterised and sequenced. This meant that no-mutant wild type comparison docking simulation data was generated. The two species in bold (*P. fluorescens* and *C. sapidus*) were characterised in-silico via Alphafold and docking simulations but their plasmids were not assembled.

Different concentrations of silver nitrate ($AgNO_3$) were added to LB agar plates, creating negative selection pressure. The concentrations were chosen based on experiments conducted to identify the MIC of BL21(DE3) cells. The screen was designed to plate the entire mutant library of MTs along with their WT variants. Colonies which exhibited growth at higher $AgNO_3$ concentrations would be characterised using sequencing, mass spec and re-screened at higher $AgNO_3$ concentrations.

Each species along with relevant mutants would also be structurally modelled using Alphafold and compared in-silico via docking simulations on AutoDock 4.2, using Ag^+ as the ligand (Figure 1a).

Through residue conservation studied by phylogenetic analysis of related MTs via Multiple Sequence Alignments (MSA) possible mutation sites for MTs would be identified to generate primers and proposals for site specific random or targeted mutagenesis.

The MT DNA was randomly mutagenized through error-prone PCR using Taq M0267, and all DNA was assembled into expression plasmids with a constitutive promoter, using level 1 Joint Universal Modular Plasmids (JUMP) assemblies, a Type II restriction endonuclease-based method (Valenzuela-Ortega M and French C., 2021). The MT constructs were N-terminally-tagged with yeast SUMO (small ubiquitin-related modifier) to reduce proteolytic degradation and enhance stability and solubility of the MTs (Li et al., 2021; Malakhov et al., 2004). The SUMO-MT fusion protein sequences were also His-tagged for potential affinity purification of the protein as a step towards biochemical and biophysical characterisation.

In this study, we gathered data for WT docking simulations in the form of Gibbs free energy per Ag^+ ion (Table 1). We also gathered data on $AgNO_3$ MIC for BL21 (DE3) cells and how MIC increases upon recombinant MT expression (Figure 3). Mutation sites for each MT were also proposed along with the generation of primers for site-specific mutagenesis (Supplementary Information S.6, S.7 & S.8).

2. Results

2.1 Determining inhibitory concentration of BL21(DE3)

To establish the MIC of untransformed BL21(DE3) and TOP10 cells, they were plated on a range of $AgNO_3$ concentrations starting with 8mg/L until a fall-off in growth was observed (16 mg/L for BL21(DE3) cells). Cells were observed forming lawns until 16 mg/L and 17 mg/L with a sharp decline after that. This allowed us to explore 16 mg/L as the starting baseline concentration for the MT expressing cells. Contrastingly, TOP10 cells did not grow on any selected concentration suggesting that their silver resistance was too low to setup a functional selection pressure (Figure 2).

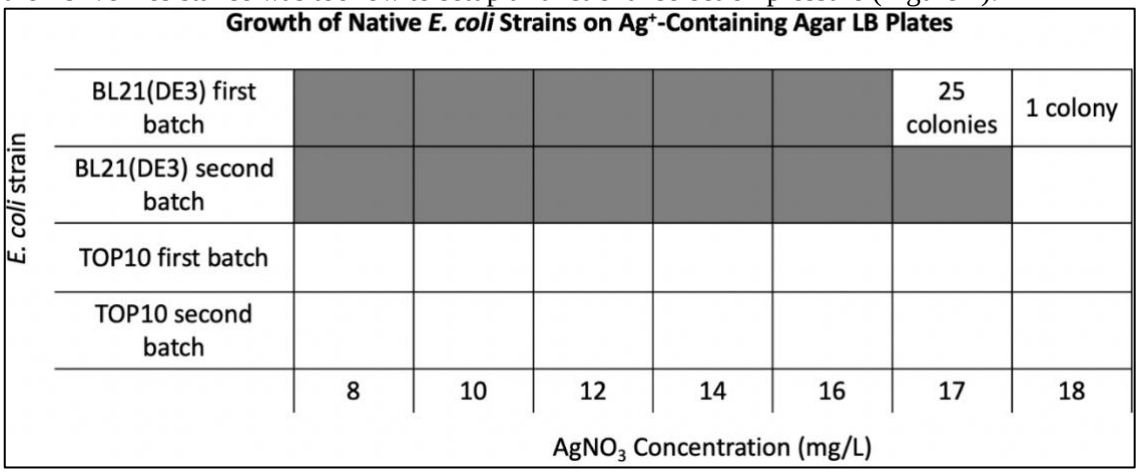

Figure 2. The cultured strains were plated in duplicate on $AgNO_3$ plates from 8-18 mg/L. The number of colonies grew on the plate was counted, with a solid colour representing a bacterial lawn and blank indicating no growth. It was observed that there is a growth fall-off at 16 mg/L for BL21(DE3) cells while the lowest concentrations of $AgNO_3$ was observed to be toxic towards TOP10 cells.

2.2 Error prone PCR mutant library generation

Error prone (EP) PCR was used to generate a mutant library of MTs (Figure 6). A higher concentration of dTTPs was used which would increase the chance of mutations with Uracil in the transcript. This is favourable for UGU and UGC as outcomes, which are the codons for cysteine (Section 4.3).

The mutated PCR products were double-stranded linear fragments of DNA which were assembled into the ORF of pJUMP29-1A(lacZ) level 1 plasmids containing a constitutive promoter (J23100), using level 0 parts (Supplementary Information S.1) following the JUMP assembly protocol (Valenzuela-Ortega and French, 2021). The same assembly method was used to generate WT MT expression plasmids.
All Level 1 plasmids were transformed into TOP10 cells and subjected to blue-white colony screening where blue colonies represent LacZ positive control. White colonies were checked for containing the insert using colony PCR (Section 4.2.2). A single WT MT expressing colony was picked and cultured to be transformed into BL21(DE3) cells for protein expression and negative selection. Similarly, a random mutant colony was picked, verified for containing the insert and cultured for BL21(DE3) transformation and subsequent selection. The mutants and wild type MT expressing cells were plated on $AgNO_3$ plates of increasing concentration (16-30 mg/L).

2.3 Negative selection for enhanced metal binding capacity

The assembled plasmids were transformed into TOP10 cells. This meant the mutant libraries were plated on blue/white colony screening plates in TOP10 cells. To transfer the DNA of each white colony on a plate to BL21(DE3) cells would not be feasible, since the MIC of TOP10 cells was not determined (Figure 2) we could not screen for the best mutant. Hence, one mutant was selected at random and transformed to our expression strain.

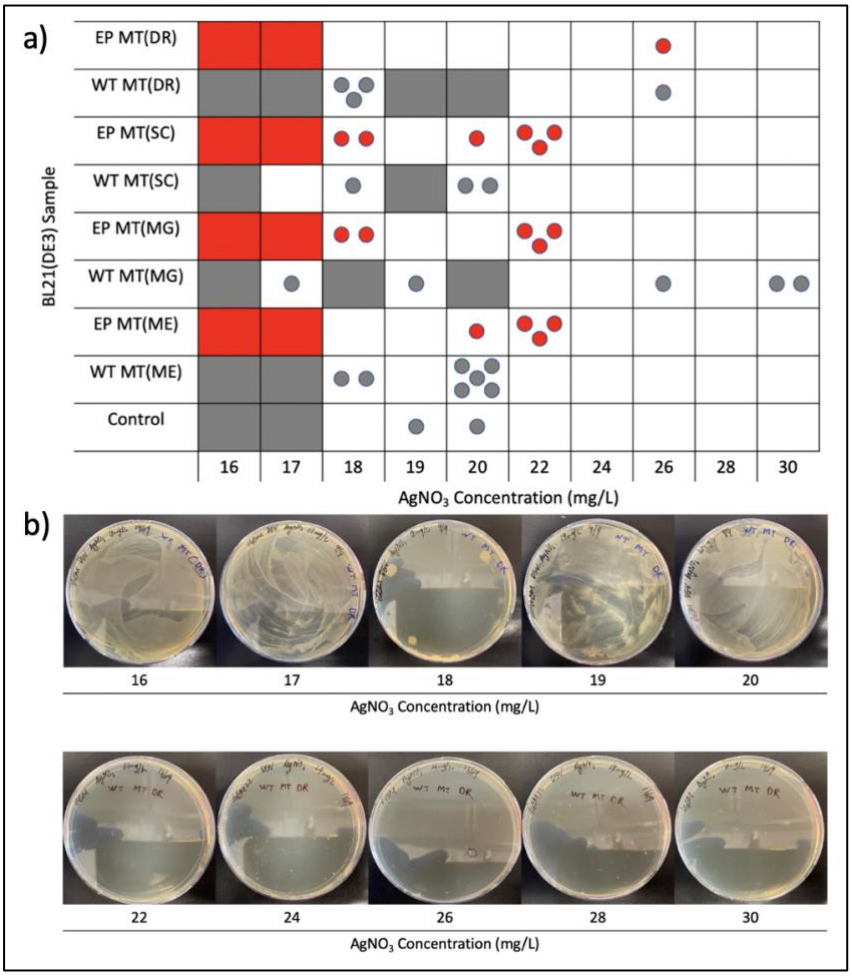

Figure 3. a) Illustrates, colony counts of BL21(DE3) recombinantly expressing MTs. In the figure, BL21 (DE3) cells expressing MTs of *Danio rerio* (DR), *Saccharomyces cerevisiae* (SC), *Mytilus galloprovincialis* (MG), and *Mytilus edulis* (ME) were plated, the wild type is shown in grey and the randomly picked mutant (EP) in red. The figure shows a significant difference in MIC between all the MTs expressing cells and the control. The figure doesn't indicate if the mutants were better than WTs or vice versa. However, some MTs grew at higher concentration but did not grow at lower concentrations. **b)** Shows an example of the raw data using WT MT DR plates. The colonies were counted and photographed for each species (Supplementary Information S.3).

MTs originating from almost all species, except for *S. cerevisiae* and *M. galloprovincialis* grew as lawns at 16 and 17 mg/L of $AgNO_3$. The results indicated that there is a sharp decrease in BL21(DE3) growth at 20 mg/L beyond which no lawns were observed for the four species of MTs shown in Figure 3a. Interestingly, in several plated samples (EP MT (DR), WT MT (DR) and WT MT (MG)) no growth was observed in lower concentrations while some colonies grew at higher concentrations.

These colonies are good candidates for sequencing analysis and re-plating at higher concentrations. Additionally, the results also indicate that a randomly selected mutant from an EP PCR library did not outperform the wildtype variant of the same species indicating that a screen of the entire mutant library is pertinent.

2.4 Docking simulations

FASTA sequences of the six MTs were taken from the NCBI database. These sequences were folded, and the Alphafold structures shown in Figure 4 were predicted. These structures were docked to Ag^{+} using AutoDock 4.2 such that the structures were hydrated and energy minimised while allowing gamma sulphurs on the sidechains of cysteines to form coordinate covalent bonds with the metal ligand (Figure 4g). The energy minimisation was done after each ligand was docked. MTs contain many cysteines however each cysteine does not carry the same binding affinity for the ligand. This was accounted for using a pass/fail metric (Supplementary Information S.12) where the passed cysteine had negative Gibbs free energy thus making the binding spontaneous.

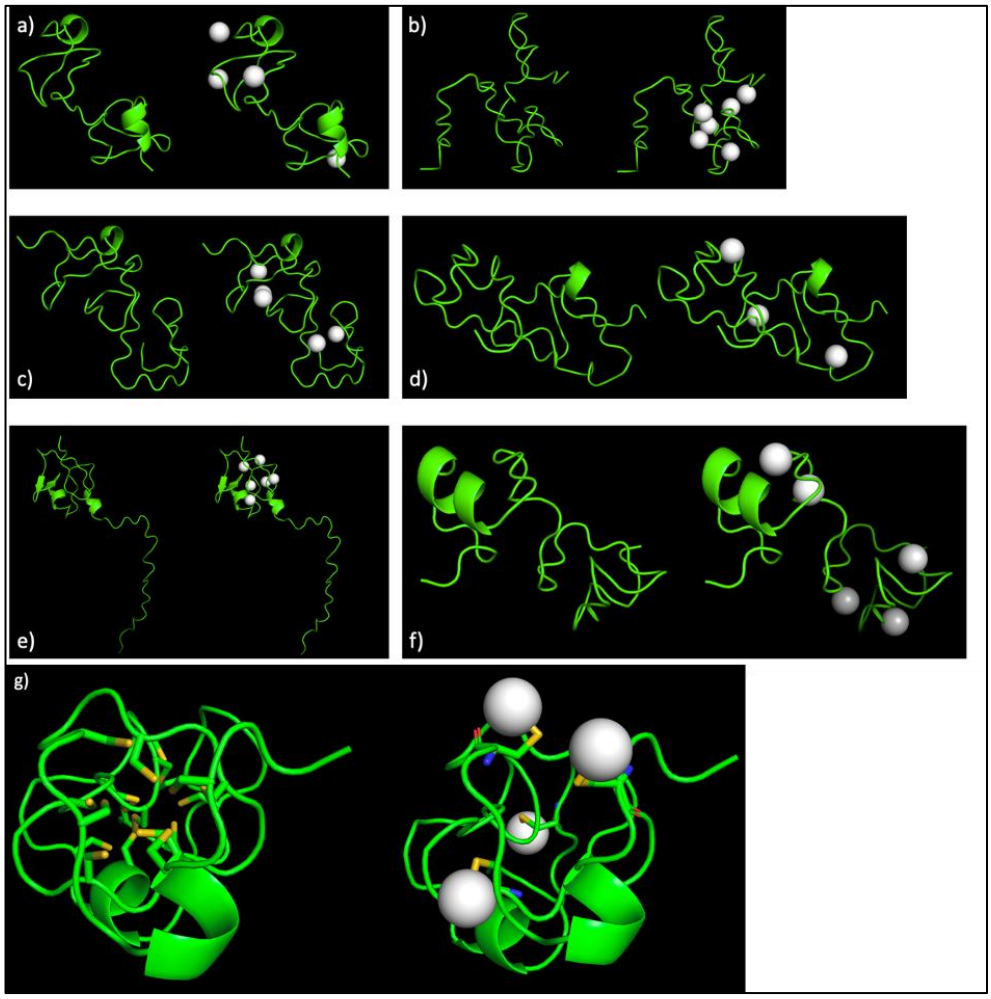

Figure 4 a-f) The structures on the left side are generated by AlphaFold using FASTA sequences, and on the right side are the Autodock-generated docking simulations of Ag+ ligands forming coordinate covalent bonds to the WT MT structures. **(a)** *Danio rerio.* **(b)** *S. cerevisiae.* **(c)** *Mytilus galloprovincialis.* **(d)** *Mytilus edulis.* **(e)** *Pseudomonas fluorescens.* **(f)** *Callinectes sapidus.* **g)** on the left is the undocked structure of *D. rerio* with all cysteine sidechains visible, the structure on the right is the docked *D. rerio* structure, which illustrates the conformational change in the gamma sulphurs upon forming coordinate covalent bonds.

Furthermore, based on the number of ligands bound per MT a score for the Gibbs free energy of binding per ion was generated for all WT MT sequences (Table 1). The data indicates that *P. fluorescens* which has the fewest number of cysteines, binds the greatest number of ions, therefore

having the lowest total Gibbs free energy and Gibbs free energy of binding per ion (-0.407 kcal/mol). This suggests that *P. fluorescens* has a high binding efficiency and affinity for Ag^+ ions. Contrastingly, MTs like *M. edulis* contain more cysteines but bind to fewer Ag^+ ions thus having a lower binding efficiency and affinity.

Table 1. In-silico modelled Gibbs free energy

Metallothionein:	Total cysteines:	Number of Ag^+ ions docked:	Total free energy of binding (kcal/mol):	Gibbs free energy of binding per ion (kcal/mol):
M. edulis	20	4	-0.83	-0.208
M. galloprovincialis	21	5	-0.85	-0.170
D. rerio	20	4	-0.58	-0.145
C. sapidus	18	5	-0.65	-0.130
P. fluorescens	9	6	-2.44	-0.407
S. cerevisiae	12	5	-1.87	-0.374

2.3 Identifying mutation sites

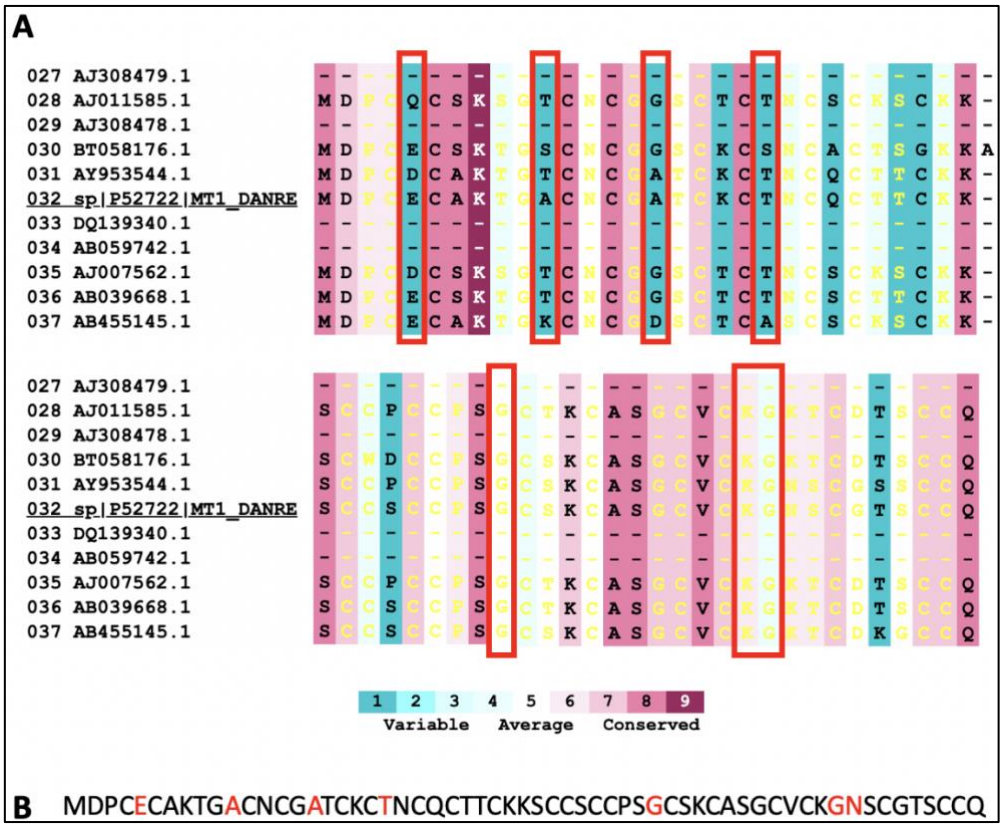

Figure 5. a) Multiple sequence alignments of the MTs were followed by conservation analysis against phylogenetically relevant MTs **b)** Shows the sequence of *Danio rerio* metallothionein, with amino acids targeted for potential mutagenesis highlighted in red.

MTs contain metal-binding motifs which typically present as:

cys-x-cys, cys-x-x-cys, x-cys-cys-x and x-cys-cys-cys-x

Here, x denotes any amino acid other than cysteine (Ziller and Fraissinet-Tachet, 2018). We hypothesised that increasing the number of these motifs in a MT molecule would increase its number of metal-binding sites as long and the protein was functionally folded.

Using Consurf, we analysed our MSA, it generated conservation scores based on phylogenetic analysis. We identified the less conserved regions between two cysteines at least 3 residues apart (Figure 5a). These less conserved sites (Figure 5b) are proposed as possible sites to explore for site-specific mutagenesis using random mutagenic methods like GeneOrator or targeted mutagenesis. We created mutagenic primers for the same (Supplementary Information S.7, S.8).

3. Discussion

As our results indicate, we did not screen the entire mutant library (Figure 3a). This was a consequence of several failed DNA assemblies and transformation into BL21 (DE3) cells directly from the JUMP assembly reaction. We observed no colony growth post-transformation, and several colony PCRs showed that the chemically competent BL21 (DE3) cells did not contain the expression plasmid for our MTs. We tried various troubleshooting measures like increasing DNA concentrations in the plasmid assembly reaction, trying different protocols to make a new batch of chemically competent BL21 (DE3) cells. Each assembly was tested via Eco R1 digestion and colony PCR. Given the unsuccessful results, we tried transforming our assemblies onto TOP10 cells (*E. coli* strain) which was successful, this made it relevant to test the $AgNO_3$ MIC of TOP10 cells, replacing BL21(DE3) in the screen. It was observed that $AgNO_3$ was significantly more toxic for TOP10 cells than BL21 (DE3) cells. No growth was observed in TOP10 cells at concentrations as low as 8 mg/L. Consequently, we were not able to establish the MIC of TOP10 cells towards $AgNO_3$ which meant that we couldn't successfully establish a starting concentration for a TOP10 cell based mutant screen. We re-designed our experimental pipeline to focus on inferring whether $AgNO_3$ toxicity was a valid method for a possible BL21(DE3) mutant screen.
For this, one random mutant MT expressing colony was taken and transformed to BL21(DE3) cells and plated on the $AgNO_3$ plates, alongside a WT variant of the same species. This result doesn't indicate if random mutagenesis is the best approach for directed evolution of MTs and other techniques involving site-specific and targeted mutagenesis should be explored.
The results (Figure 3a) show that MT expression does have an impact on the overall MIC of the cell. However, it is difficult to conclude whether the rise in MIC was due to outliers, or metal bioaccumulation. Additionally, this change could be due to cells down-regulating metal transporter proteins, faulty plates with precipitation, or expression of other proteins. To ensure that the original screening hypothesis holds true, the selection needs to be done using controls for all the above stated factors along with the necessary repetition for more accurate data. Protein expression was also not factored into the results, survival at higher concentration for each MT could be because the MTs are chelating more metals per molecule or because the protein expression of 1 MT species is significantly higher than others.

The selection results indicate that the mutants selected did not outcompete WTs for survival, to validate the scope of this screen as a tool to study MTs for bioaccumulation, it would be necessary to do a complete mutant library screen in BL21(DE3) cells. The relevant mutants should be characterised by mass-spec, sequenced, and rescreened along with comparative docking simulations (Figure 1a).

The docking simulations (Figure 4) and Table 1 was generated using assumptions. The maximum Gibbs free energy (Torsional free energy) was kept constant at 0.60 kcal/mol (Supplementary Information S.13) for all MT species because new atom types cannot be used to calculate the Root Mean Square Deviation (RMSD) of the ligand. This impacts the overall accuracy of the docking.
The overall experimental output showcased the shift in survival between untransformed BL21 (DE3) cells the MT expressing cells, *P fluorescens,* showed more "efficient" binding based on the data from Table 1, however, it was never tested experimentally due to flaws in the DNA construct along with *C. sapidus* which wasn't tested due to a shortage of resources.

This study shows that there is potential in exploring MTs as an option when considering biotechnological solutions towards problems as scary as the water pollution crisis in Ghana. The novel

screening method explored here has not been characterised fully but leaves room for further directed evolution experiments and a platform for doing so has also been provided with the proposal for alternate methods of random site-specific mutagenesis.

4. Materials and Methods

4.1.1 Chemicals and materials

Designed DNA of MT with other parts and the primers were synthesized by Integrated DNA Technologies (Leuven, Belgium) and designed on Benchling. dNTPs and enzymes including Taq M0267 DNA polymerase, BsmBI andT4 ligase were purchased from New England Biolabs (Hitchin, United Kingdom). QIAprep Spin Miniprep Kit and QIAquick PCR purification kits were purchased from QIAGEN (Hilden, Germany). $CaCl_2$, $MgCl_2$, $AgNO_3$, and $ZnCl_2$ were purchased from Sigma-Aldrich.

TOP10 and BL21 (DE3) competent cells were made in the lab. The plasmid backbone pJUMP18-Uac and pJUMP29-1A(lacZ) used in JUMP assembly were kindly provided by Marcos Valenzuela-Ortega and Chris French's laboratory, The University of Edinburgh.

4.1.2 Competent cell preparation

TOP10 and BL21 (DE3) competent cells were prepared by taking 1mL liquid culture from overnight cultures into 100mL LB culture, incubated at 37 °C, 200rpm until OD600 =0.4-0.6. The cultures were transferred to 50mL falcon tubes and left on ice for 30 mins, followed by 4000 x g centrifugation at 4°C for 5 mins. Cells were resuspended gently in 25mL 0.1M ice cold $MgCl_2$ then left on ice for 30 mins and centrifuged at 4000 x g (4°C for 5 mins). The same was repeated for resuspension in 0.1M $CaCl_2$ (30 mins ice, followed by 4000 x g centrifugation 5mins at 4°C). The cells were then resuspended in 1.25ml ice cold $CaCl_2$/glycerol solution (1.7 mL 0.1 M $CaCl_2$, 0.3 ml 100 % glycerol). 100ul aliquots were made and flash frozen on dry ice to then be stored at – 80 °C.

4.1.3 $AgNO_3$ plates preparation

$AgNO_3$ stock solution was made with the concentration of 0.256 mg/mL. The stock solution was made in a dark room due to the light-reactive nature of silver. Additionally, steps were taken to optimise adding $AgNO_3$ to molten LB agar at the correct temperature (50°C) such that, silver did not precipitate out in a dark room.

Table 2. Volume of $AgNO_3$ stock solution per 50 mL of LB for gradient plates

$AgNO_3$ concentration (mg/L)	$AgNO_3$ stock solution volume (μL)
8	1.563
10	1.953
12	2.344
14	2.734
16	3.130
17	3.330
18	3.520
19	3.720
20	3.910
22	4.300
24	4.690
26	5.080
28	5.470
30	5.860

Adding the above stated volumes of $AgNO_3$ to 50 mL LB agar produces 2 silver plates of 25mL each.

4.2 JUMP Assembly

4.2.1 Level 0 Parts DNA parts domestication

Based off the 6 species for which MT protein structure and function is well-known, MT sequences were designed to contain a SUMO-tag for stability and 6-his-TEV for tagging (Ma *et al.* 2018). The assembly was performed on the DNA parts with 1 cycle at 42°C for 15 min; 30 cycles at 42°C for 3 min, 16°C for 3 min; 1 cycle at 55°C for 15 min, 80°C for 5 min, then held at 10°C. The products were domesticated into JUMP acceptor vector pJUMP18-Uac (20 fmol/µL) via BsmBI cutting and T4 ligase annealing, producing the level 0 plasmids (Supplementary Information S.1). The level 0 plasmids were transformed into TOP10 competent cells and selected with LB plates containing ampicillin (100µg/ml). Parts were miniprepped from successful level 0 plasmid-containing overnight cultures (Valenzuela-Ortega and French, 2021).

4.2.2 Level 1 Assembly

The level 0 parts were assembled using an extended version of the original level 1 assembly protocol (Supplementary Information S.1). The assembly was performed with 1 cycle of 42 °C for 15 minutes; 30 cycles of 42 °C for 3 minutes and 16 °C for 3 minutes; followed by a single cycle of 55 °C for 15 minutes and 80 °C for 5 minutes, then held at 10 °C. The level 0 parts were assembled into a pJUMP29-1A(lacZ) acceptor vector cut by BsaI and ligated by T4 ligase (Valenzuela-Ortega and French, 2021). The assemblies were transformed into competent *E. coli* cells that were then plated on LB plates containing kanamycin (100 µg/mL), X-gal (8 µg/mL) and IPTG, which allowed for distinguishing colonies containing successfully assembled plasmids for miniprepping.

4.3 Mutant library generation (Error prone PCR)

To induce mutations on MT, EP PCR Taq M0267 was done with all 5 types of MT level 0 plasmids (Figure 6). For *Mytilus edulis*, specifically designed primers were used (Forward: CGTCTCGGTCTCCTTCGATGCC; Reverse: CGTCTCAGGTCTCGAAGCCTACTAGC), and all other MT types used PS1 (Forward: AGGGCGGCGGATTTGTCC) and PS2 (Reverse: GCGGCAACCGAGCGTTC), designed for the pJUMP29-1A(lacZ) backbone plasmids. 1.475 µl of 2.95 µM $MgCl_2$ to reduce Taq M0267 fidelity, a non-proofreading polymerase (Wilson and Keefe, 2001). dNTP concentrations were varied for each base (3.5 mM dATP, 4 mM dCTP, 6mM dGTP, 13.5 mM dTTP) to promote mutations, the concentrations of dTTP were in excess, as increasing Thymidine mutations would translate into more uracil-rich areas in the mRNA transcript. UGU and UGC encode cysteine, so by increasing uracil, we attempted to increase cysteine richness to increase MT metal-binding properties. EP PCR was performed with 1 cycle at 95°C for 60s; 25 cycles at 95°C for 30s, 1 cycle at 72°C for 45s, 1 cycle at 68°C for 90s, elongation at 68°C for 5 mins, then held at 4°C. Mutant MT plasmids were then purified and kept at -18°C.

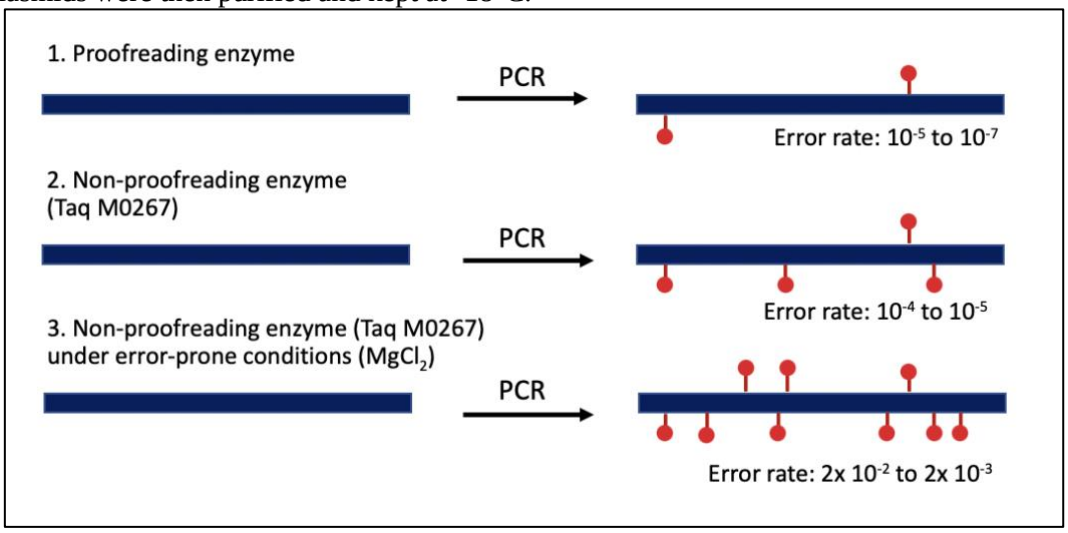

Figure 6. Comparison of Error-Prone PCR conditions to fidelity of standard PCR. Addition of *Taq* M0267 reduces fidelity. In the presence of $MgCl_2$, error rate is also increased to increase the overall mutation rate (Adapted from Wilson and Keefe, 2001).

4.4 Plasmid verification

Successful level 1 assemblies were verified with colony PCR. Each type of MT SUMO and 6-his-TEV-containing level 0 plasmid was assembled into level 1 vector pJUMP29-1A(lacZ) (20 fmol/µL) acceptor plasmids using JUMP level 1 assembly (Valenzuela-Ortega M and French C., 2021). The level 1 assembled MT plasmids of each species were transformed into BL21 (DE3) competent cells and selected with LB kanamycin (50µg/mL) plates. From level 1 part-containing TOP10 cells, white colonies were picked from Blue-White colony screening and verified by colony PCR. In a 25µl reaction tube the following were added: PS1 (2.5µL), PS2 (2.5µL) primers (1µM), dNTP mix (0.5µL, 10mM) dNTP mix, 5x Green GoTaq Reaction buffer (5µL), GoTaq G2 DNA polymerase (0.125 µL), DNA template (5µL) (with the initial denaturation step at 95 °C for 3 minutes, 30 cycles of 95 °C for 15 seconds, 55 °C for 15 seconds and 72 °C for 30 seconds, followed by a final extension at 72 °C for 5 minutes. The MT-containing white colonies with verified plasmids were reinoculated into 10 mL LB overnight at 37°C. Level 1 MT plasmids were purified from liquid culture.

Digestions to check for correctly assembled DNA were done in 20 µL reactions with 2 µL of rCutSmart Buffer, 1 µL *EcoRI* Heat Inactivated and 100-200ng DNA, left for 2h at 37°C. The product of both the digestion and colony PCR were run on an agarose gel.

4.5 Transformation of MT plasmids

10 µL of plasmid DNA was added to thawed aliquots of BL21 (DE3) competent cells then left on ice for 30 minutes. The cells were then heat shocked at 42°C for 30 seconds followed by 30 seconds on ice. 1mL SOC media was added to then incubate them at 37°C, 500 rpm for 45 mins. 100 µL of transformed cells were then plated on respective ampicillin/kanamycin LB plates. For clearer colonies, aliquots were spun down at 13000 g, resuspended in 100 µL SOC and then was plated. Transformed cell-containing plates were incubated over night at 37°C.

4.6 Negative selection

4.6.1 BL21(DE3) silver tolerance test with $AgNO_3$ plates

Mutations in gram negative bacteria can increase silver tolerance up to 256 mg/L (Randall C. P. et al., 2015). To understand the exact silver tolerance of the BL21(DE3) cells that were to be used for the MT expression and screening, a $AgNO_3$ tolerance test of wild-type BL21(DE3) was carried out with concentrations ranging from 8mg/L to 256 mg/L, with every subsequent concentration being twice that of the previous one. Afterwards, silver nitrate tolerance was further tested between 16 mg/L and 20 mg/L.

4.6.2 Negative selection pressures identifying improved MT

Transformed BL21 (DE3) cell lines that containing either native or mutant metallothionein were grown on $AgNO_3$ gradient plates for 12h at 37°C. Native metallothionein were used as control and compared with the mutant metallothionein plates. Colony growth on $AgNO_3$ plates nearing inhibitory concentrations were indicative of BL21 (DE3) cells with enhanced metal binding capacity, which was assumed as having improved MT activity.

4.7 Bioinformatics

4.7.1 Multiple Sequence Alignment

The sequences for all the MTs were obtained from the NCBI database. The Open Reading Frames (ORFs) were identified, and some reverse transcribed sequences were converted to anti-sense DNA using python. These sequences were then translated in-silico. The translated sequences were analysed using Multiple Sequence Alignment (MSA) with sequences of phylogenetically similar MTs. This was determined based on the available data for MTs related to each species. For *P. fluorescens* the sequences were limited to phylum and for *S. cerevisiae* the family, for the other four, sequences of MTs present within their phylogenetic class were used. The outliers were removed, and the aligned results were run on ConSurf to generate conservation scores for each residue using the selected MTs as the query sequence. Based on literature, optimal cysteine-metal binding motifs were selected. The residues which were heavily conserved in the phylogenetic analysis were assumed to be essential for MTs structure and function and were not modified (Supplementary Information S.6).

4.7.2. Alphafold structure generation

A FASTA file was generated for each MT. These FASTA sequences were processed and modelled using Alphafold on a computing cluster at The University of Edinburgh.

4.7.3 AutoDock 4.2 docking simulation

Autodock 4.2 Docking Simulations Ligand PDB files were modified for flexible side chain covalent docking with AutoDock's prepareCovalent.py. The PDBs generated from this as well as Metallothionein PDBs were prepared using MGLTools prepare_receptor4.py. Flexible bonds were identified using MGLTools prepare_flexreceptor4.py. Grid parameter files were generated using MGLTools prepare_gpf4.py with grids centered on the ligand, incrementing 20 grid points in all dimensions, and docking parameter files were generated using prepare_dpf4.py (Supplementary Information S.11). Parameter files were modified to use a new atom parameter file containing Silver. AutoGrid was used to calculate atomic affinities, and AutoDock 4.2 was used to perform docking. The docked coordinates of the silver ion and the corresponding gamma sulphur were extracted from the resulting docking log files and inputted into the original structure if the free energy of binding was below 0.60 kcal/mol, and the original gamma sulphur was removed (Supplementary Information S.13).

4.7.4 Docking simulation automation

The docking simulations done using AutoDock 4.2 were also automated. This process was automated using Unix. Each gamma sulphur in cysteine sidechains of each metallothionein were extracted, and all processes in the docking simulations were run in parallel for each gamma sulphur. A consensus structure was generated for each metallothionein with the approaches mentioned in the previous section. Full annotated scripts are available in the supplementary methods (clean_automation.sh) (Supplementary Information S.11).

5. Author Contributions

D.V., M.V.D.A., W.M., X.X., S.S and Z.L. designed experiments. N.L. and C.F. provided advice and expertise on experimental design, data analysis and manuscript editing. D.V., X.X., S.S. and D.S. performed experiments. M.V.D.A, D.B.J., S.S. and D.V. did computational analysis. M.V.D.A., A.W., M.S. provided bioinformatics, and modelling support. D.V., D.B.J., X.X., S.S., D.S. and M.V.D.A. analysed data and wrote the manuscript.

6. Acknowledgments

We would like to thank Dr Nadanai Laohakunakorn and Prof Chris French for their overall supervision and guidance. We would like to thank Dr Heather Barker, Prof French and Giovanni Maddalena for providing us with laboratory space, experimental equipment and reagents. We would like to thank Marcos Valenzuela-Ortega for providing us with JUMP parts. We appreciate Arin Wongprommoon, Giovanni Maddalena, Michael Stam, Surendra Yadav and Dr Anton Puzorjov for their feedback and support at every stage of this project. We would also like to acknowledge the efforts of the UHAS-Ghana team members who collaborated with us on the iGEM project and provided us with a human practices-based direction for our lab work.

7. Competing Interests

The authors declare no competing interests.

8. Supplementary Information

Supplementary information submitted online.

9. References

Butt, T. and Ecker, D., 1987. Yeast metallothionein and applications in biotechnology. Microbiological Reviews, 51(3), pp.351-364. DOI: 10.1128/mr.51.3.351-364.1987

Currin, A., Kwok, J., Sadler, J., Bell, E., Swainston, N., Ababi, M., Day, P., Turner, N. and Kell, D., 2019. GeneORator: An Effective Strategy for Navigating Protein Sequence Space More Efficiently through Boolean OR-Type DNA Libraries. ACS Synthetic Biology, 8(6), pp.1371-1378. DOI: 10.1021/acssynbio.9b00063

Chopra, I., 2007. 'The increasing use of silver-based products as antimicrobial agents: a useful development or a cause for concern?', Journal of antimicrobial chemotherapy, 59(4), pp. 587-590. DOI: 10.1093/jac/dkm006

Chan, K., Ku, L., Chan, P. and Cheuk, W., 2006. Metallothionein gene expression in zebrafish embryo-larvae and ZFL cell-line exposed to heavy metal ions. Marine Environmental Research, 62, pp. S83-S87. DOI: 10.1016/j.marenvres.2006.04.012

Coyle, P., Philcox, J. C., Carey, L. C. and Rofe, A. M., 2002. 'Metallothionein: the multipurpose protein', Cellular and molecular life sciences: CMLS, 59(4), pp. 627-647. DOI: 10.1007/s00018-002-8454-2

De Martinez Gaspar Martins, C. and Bianchini, A., 2009. Metallothionein-like proteins in the blue crab Callinectes sapidus: Effect of water salinity and ions. Comparative Biochemistry and Physiology Part A: Molecular & Integrative Physiology, 152(3), pp.366-371. DOI: 10.1016/j.cbpa.2008.11.005

Habjanič, J., Chesnov, S., Zerbe, O. and Freisinger, E., 2019. Impact of naturally occurring serine/cysteine variations on the structure and function of Pseudomonas metallothioneins. Metallomics, 12(1), pp.23-33. DOI: 10.1039/c9mt00213h

Leignel, V. and Laulier, M., 2006. Isolation and characterization of Mytilus edulis metallothionein genes. Comparative Biochemistry and Physiology Part C: Toxicology & Pharmacology, 142(1-2), pp.12-18. DOI: 10.1016/j.cbpc.2005.09.011

Li, X., Ren, Z., Crabbe, M., Wang, L. and Ma, W., 2021. Genetic modifications of metallothionein enhance the tolerance and bioaccumulation of heavy metals in Escherichia coli. *Ecotoxicology and Environmental Safety*, 222, p.112512. DOI: 10.1016/j.ecoenv.2021.112512

Ma, W., Li, X., Wang, Q., Ren, Z., Crabbe, M. and Wang, L., 2019. Tandem oligomeric expression of metallothionein enhance heavy metal tolerance and bioaccumulation in Escherichia coli. *Ecotoxicology and Environmental Safety*, 181, pp.301-307. DOI: 10.1016/j.ecoenv.2019.06.022

Malakhov, M., Mattern, M., Malakhova, O., Drinker, M., Weeks, S. and Butt, T., 2004. SUMO fusions and SUMO-specific protease for efficient expression and purification of proteins. *Journal of Structural and Functional Genomics*, 5(1/2), pp.75-86. DOI: 10.1023/B:JSFG.0000029237.70316.52

OLAFSON, R., 2009. Prokaryotic metallothionein. International Journal of Peptide and Protein Research, 24(3), pp.303-308. DOI: 10.1111/j.1399-3011.1984.tb00957.x

Olafson, R. W., McCubbin, W. D. and Kay, C. M., 1988. 'Primary- and secondary-structural analysis of a unique prokaryotic metallothionein from a Synechococcus sp. cyanobacterium', Biochemical journal, 251(3), pp. 691-699. DOI: 10.1042/bj2510691

Oppong Afum, B., 2016. Heavy Metal Pollution in the Birim River of Ghana. International Journal of Environmental Monitoring and Analysis, 4(3), p.65. DOI: 10.11648/j.ijema.20160403.11

Randall, C., Gupta, A., Jackson, N., Busse, D. and O'Neill, A., 2015. Silver resistance in Gram-negative bacteria: a dissection of endogenous and exogenous mechanisms. Journal of Antimicrobial Chemotherapy, 70(4), pp.1037-1046. DOI: 10.1093/jac/dku523

Scheuhammer, A. M. and George Cherian, M., 1986. Quantification of metallothionein by silver saturation. Toxicology and Applied Pharmacology, 82(3), pp.417-425. DOI: 10.1016/0041-008X(86)90277-2

Schwarzenbach, R. P., Egli, T., Hofstetter, T. B., Von Gunten, U. and Wehrli, B., 2010. 'Global Water Pollution and Human Health', Annual review of environment and resources, 35(1), pp. 109-136. DOI: 10.1146/annurev-environ-100809-125342

Valenzuela-Ortega, M. and French, C., 2021. Joint universal modular plasmids (JUMP): a flexible vector platform for synthetic biology. Synthetic Biology, 6(1). DOI: 10.1093/synbio/ysab003

Vergani, L., Grattarola, M., Grasselli, E., Dondero, F. and Viarengo, A., 2007. Molecular characterization and function analysis of MT-10 and MT-20 metallothionein isoforms from Mytilus galloprovincialis. Archives of Biochemistry and Biophysics, 465(1), pp.247-253. DOI: 10.1016/j.abb.2007.05.023

Wilson, D. S. and Keefe, A. D., 2001. 'Random mutagenesis by PCR', Current protocols in molecular biology (Print), 8, pp. Unit8.3. DOI: 10.1002/0471142727.mb0803s51

Xu, X., Duan, L., Yu, J., Su, C., Li, J., Chen, D., Zhang, X., Song, H. and Pan, Y., 2018. Characterization analysis and heavy metal-binding properties ofCsMTL3inEscherichia coli. FEBS Open Bio, 8(11), pp.1820-1829. DOI: 10.1002/2211-5463.12520

Ziller, A. and Fraissinet-Tachet, L., 2018. Metallothionein diversity and distribution in the tree of life: a multifunctional protein. Metallomics,10(11), pp.1549-1559. DOI: 10.1039/c8mt00165k